NanoImpact 37 (2025) 100539

Contents lists available at ScienceDirect

NanoImpact

journal homepage: www.elsevier.com/locate/nanoimpact

Research Paper

The dispersion method does not affect the *in vitro* genotoxicity of multi-walled carbon nanotubes despite inducing surface alterations

Michael J. Burgum [a], Víctor Alcolea-Rodríguez [b,1], Hanna Saarelainen [c,1], Raquel Portela [b], Julián J. Reinosa [d], José F. Fernández [d], Verónica I. Dumit [e], Julia Catalán [c,f], Felice C. Simeone [g], Lara Faccani [g], Martin J.D. Clift [a], Stephen J. Evans [a], Miguel A. Bañares [b], Shareen H. Doak [a,*]

[a] *In Vitro Toxicology Group, Faculty of Medicine, Health and Life Sciences, Institute of Life Sciences, Swansea University Medical School, Singleton Park, Swansea SA2 8PP, UK*
[b] *Institute of Catalysis and Petrochemistry, CSIC, C/Marie Curie, 2, E-28049 Madrid, Spain*
[c] *Finnish Institute of Occupational Health, Box 40, Työterveyslaitos, 00032 Helsinki, Finland*
[d] *Instituto de Cerámica y Vidrio, CSIC, c/Kelsen, 5, E-28049 Madrid, Spain*
[e] *German Federal Institute for Risk Assessment (BfR), Department of Chemical and Product Safety, Germany*
[f] *Department of Anatomy Embryology and Genetics, University of Zaragoza, c/Miguel Servet, 177, E-50013 Zaragoza, Spain*
[g] *Institute for Science, Sustainability and Technology of Ceramics-ISSMC-CNR, via Granarolo 64, 48018 Faenza, Italy*

A R T I C L E I N F O

Editor: Bernd Nowack

Keywords:
CNTs
Oxidative potential
In vitro genotoxicity
Secondary genotoxicity
NanoGenoTox

A B S T R A C T

Multi-walled carbon nanotubes (MWCNTs) are a desirable class of high aspect ratio nanomaterials (HARNs) owing to their extensive applications. Given their demand, the growing occupational and consumer exposure to these materials has warranted an extensive investigation into potential hazards they may pose towards human health. This study utilised both the *in vitro* mammalian cell gene mutation and the cytokinesis-blocked micronucleus (CBMN) assays to investigate genotoxicity in human lymphoblastoid (TK6) and 16HBE14o$^-$ human lung epithelial cells, following exposure to NM-400 and NM-401 MWCNTs for 24 h. To evaluate the potential for secondary genotoxicity, the CBMN assay was applied on a co-culture of 16HBE14o$^-$ with differentiated human monocytic (dTHP-1) cells. In addition, two dispersion methods (NanoGenoTox *vs.* high shear mixing) were utilised prior to exposures and in acellular experiments to assess the effects on MWCNT oxidative potential, aspect ratio and surface properties. These were characterized *in chemico* as well as by electron microscopy and Raman spectroscopy. Structural damage of NM-400 was observed following both dispersion approaches; Raman spectra highlighted greater oxidative transformation under probe sonication as opposed to high shear mixing. Despite the changes to the oxidative potential of the MWCNTs, no statistically significant genotoxicity was observed under the conditions applied. There was also no visible signs of cellular internalisation of NM-400 or NM-401 into either cell type under the test conditions, which may support the negative genotoxic response. Whilst these HARNs may have oxidative potential, cells have natural protective mechanisms for repairing transient DNA damage. Therefore, it is crucial to evaluate biological endpoints which measure fixed DNA damage to account for the impact of DNA repair mechanisms.

1. Introduction

Multi-walled carbon nanotubes (MWCNTs) have extensive applications in the biomedical and industrial fields, this is mostly noticeable in applications such as bone tissue regeneration, energy storage, water treatment, and sensors (Pei et al., 2019; Schnorr and Swager, 2011; Rahman et al., n.d.; Saliev, 2019). The inevitable occupational and consumer exposure to these high aspect ratio nanomaterials (HARNs) maintains the heightened concern as to the risk they pose to human health, described in the literature (Alarifi et al., 2014; Alarifi and Ali, 2015; Aldieri et al., 2013; Asakura et al., 2010; Di Cristo et al., 2019; Johnston et al., 2010; Poland et al., 2008; Sabido et al., 2020; Fenoglio et al., 2008).

Despite the great effort devoted to understanding HARN fate (*in vivo*)

* Corresponding author.
E-mail address: s.h.doak@swansea.ac.uk (S.H. Doak).
[1] These authors contributed equally.

https://doi.org/10.1016/j.impact.2024.100539
Received 10 September 2024; Received in revised form 17 December 2024; Accepted 18 December 2024
Available online 21 December 2024

and the *in vitro* mechanism of action that may contribute to their harmful effects, there are gaps in our knowledge, specifically pertaining to *in vitro* MWCNT mutagenicity (point mutation induction) in human-derived models and deducing whether MWCNTs can promote secondary mechanisms of genotoxicity in relevant lung models. Therefore, gaining a thorough understanding of these topics would give us a deeper insight into the human health hazard associated with these HARNs when considering the inevitable exposure at an occupational or consumer level. Furthermore, the concept of 'true' exposure concentration and the difficulty to achieve it is often highlighted regarding MWCNTs. HARNs must be dispersed before testing their toxicity *in vitro* or *in vivo*, but common dispersion techniques such as the probe sonicator have more regularly been tested with hydrophilic nanomaterials, such as metal oxides, than with hydrophobic nanomaterials like MWCNTs, which are not readily wetted with pure water and, thus, require more intricate approaches to achieve a stable dispersion. For instance, two studies from the same group dispersed MWCNT-7 with a Branson Sonifier mounted with a disrupter horn and found that only 7 % and 12 % of the administered 100 μg/ml dose was deposited after 3 and 24 h in 10 % FBS-supplemented media (Wils et al., 2021). A similar suspension protocol yielded a 25 % deposition dose for MWCNT-7 and NM-400 in cell culture media after 24 h (Di Ianni et al., 2021).

The aim of this study was therefore two-fold; firstly, to compare two different dispersion approaches (the NanoGenoTox protocol, based on sonication, and high-shear mixing, a sonication-free alternative) for their capacity to efficiently disperse MWCNTs but also induce physicochemical changes. Two types of reference MWCNT materials, NM-400 and NM-401 from the Joint Research Centre (JRC) of the European Commission, were selected for the study, given they have been thoroughly characterized. Secondly, the study was aimed at evaluating the *in vitro* genotoxicity of the dispersed MWCNTs in human-derived cell lines to offer a novel insight as to whether the dispersion approach can influence the genotoxicity profile of MWCNTs. Two genotoxicity tests to measure different forms of fixed DNA damage, each of which has test guidance (TG) protocols published by The Organisation for Economic Co-Operation and Development (OECD), were used to identify the type of primary damage induced by MWCNTs; namely, the *in vitro* mammalian cell gene mutation assay (OECD TG No. 476) for the detection of point mutations, and the *in vitro* mammalian cell micronucleus assay (OECD TG No. 487) for the detection of chromosomal damage (OECD, 2016; OECD, "Test No., 2016). Subsequently, the induction of secondary mechanisms of genotoxicity were evaluated through the use of co-cultures of 16HBE14o^{-} and differentiated human monocytic cells (Evans et al., 2019; Burgum et al., 2021). Finally, the oxidant reactivity of MWCNT was assessed to unravel the relation between structure-reactivity-toxicity (Alcolea-Rodriguez et al., 2024a).

2. Materials and methods

2.1. Multi-walled carbon nanotubes and preparation of suspensions

NM-400 and NM-401 MWCNT powder samples and their general physicochemical characterisation were provided by the Joint Research Centre (JRC, Ispra, Italy) (Rasmussen et al., 2014). Stock suspension of these reference MWCNT materials were prepared by following three different dispersion protocols: NanoGenoTox, high shear mixing and magnetic stirring. Additionally, the stabilization of the suspensions during 24 h was studied by using Turbiscan equipment.

2.1.1. NanoGenoTox dispersion protocol

Handling and dispersion using the NanoGenoTox protocol was carried out as described by Jensen *et al* in 2011 (C. P. A et al., n.d.). Briefly, the NM-400 and NM-401 samples were weighed out (15.36 mg) into glass scintillation vials using the OHAUS Explorer Semi-Micro Balance housed in a WAYSAFE (#GP1540). In sterile conditions, the materials were pre-wetted with 30 μl of ethanol and then 970 μl 0.05 % bovine serum albumin (BSA) solution were added to each vial. The final volume (6 ml) and CNT concentration (2.56 mg/ml) was obtained by adding 5 ml 0.05 % BSA solution. Each sample was then independently sonicated using a 550 W, 20 kHz Branson Sonifier S—450D (Branson Ultrasonics Corp, USA). The scintillation vials were always sonicated atop an ice bath and the probe tip cleaned in 70 % ethanol following the sonication period. Immediately prior to exposure, the scintillation vials were vortexed for 30s.

2.1.2. High shear mixing dispersion protocol

The NM-400 and NM-401 samples were added to Milli-Q water under stirring at 800 rpm using a Dissolver DSV-SL-1 with a cordless disc from Lleal (Granollers, Spain) and kept at rest for 48 h. The suspension was then homogenised using an Ultra-turrax disperser T-25 (IKA-Werke GmbH & Co. KG, Stuffen, Germany) at 11,000 rpm and finally dispersed in a Microfluidizer LM-10 from Microfluidics (Westwood, USA) applying a pressure of 12,000 PSI. Immediately prior to exposure, the samples underwent probe sonication for 30s using the Branson Sonifier S—450D (Branson Ultrasonics Corp, USA) at the same settings applied in the NanoGenoTox protocol.

2.1.3. Dispersion by magnetic stirring

A total of 1 g NM-400 and NM-401 were directly added to vials containing 10 mL of Milli-Q water and a magnetic stir bar to obtain 1 mg/mL suspensions by continuous agitation at 500 rpm for 1 h.

2.2. Physicochemical characterisation

2.2.1. Raman spectroscopy

NM-400 and NM-401 before and after dispersion were characterized using a Renishaw InVia Qontor micro-Raman spectrometer with a 514 nm excitation line laser and a 20× microscope objective (1.5 mW laser power). Some drops of the CNT dispersions were dropped onto a microscope glass slide, dried at room temperature, and analysed at 60 different positions, generating a representative sampling. Each spectrum consisted of 10 accumulations of 3 s.

2.2.2. Scanning electron microscopy (SEM)

NM-400 and NM-401 before and after dispersion were characterized by field emission scanning electron microscopy (FE-SEM) in a high-resolution FEI Nova Nano-SEM 230 column microscope with Schottky filament and secondary and backscattered electron detectors. Some drops of the MWCNT dispersions were dropped onto an Al support, dried at room temperature, and then analysed by FE-SEM without metallization.

2.2.3. Dissolution rate

The dissolution rate of various ions present as impurities in the selected MWCNT samples were assessed by ICP-OES in Milli-Q water suspensions at a concentration of 100 μg/mL prepared by the three dispersion protocols tested in this study. Aliquots of 20 mL were sampled and filtered (0.45 μm) immediately after dispersion (at time zero) and after 24 h. A Milli-Q water sample served as the blank.

2.3. Acellular probe reactions for oxidative potential evaluation

We estimated the oxidative potential of the MWCNTs by measuring their ability to generate ROS (*N*-dimethyl-4-nitrosoaniline oxidation by OH°) and to consume thiol-based antioxidants, *i.e.*, glutathione (by species other than ROS), cysteine (relevant for the oxidative damage to proteins) and dithiothreitol (unspecific) in an acellular setting.

2.3.1. Preparation of acellular probe reactants

Phosphate buffer solution (PBS) powder, glutathione (GSH) (pharmaceutical secondary standard), L-Cysteine (Cys) ≥ 98 %, *N*, *N*-Dimethyl-4-nitrosoaniline (RNO), 5,5′–dithio-bis-(2-nitrobenzoic acid)

(Ellman reagent) 99 %, ethylenediaminetetraacetic acid (EDTA) anhydrous ≥98 %, and hydrogen peroxide (H_2O_2) solution 30 % (*w*/w) in water were purchased from Sigma Aldrich (Italy). Dithiothreitol (DTT) was purchased from Thermo Scientific™. The reagents were used as received.

2.3.2. Dithiothreitol oxidation

The DTT assay was adapted from Alcolea-Rodriguez et al. (Alcolea-Rodriguez et al., 2024b). Briefly, the MWCNTs were dispersed (200 μg/ml) in 1 mM phosphate buffer by different protocols and mixed with an equal amount of 100 μM dithiothreitol to reach a final volume of 6 ml. After one hour of incubation at 37 °C under stirring (500 rpm) the test materials were removed by filtration before adding an equal volume of 1 mM Ellman's reagent (5,5′-dithiobis-(2-nitrobenzoic acid), DTNB) to quantify the non-oxidized DTT. In parallel, DTT in phosphate buffer without NM was incubated under the same conditions to subtract the DTT consumed by direct reaction without catalyst. DTT oxidation by hydrogen peroxide 30 % (*w*/w) in H_2O was used as a positive control. The oxidative potential is expressed as normalized index of oxidant generation (NIOG) using hydrogen peroxide as a positive control of DTT depletion or as DTT reaction rate based on surface area or on the number of active sites.

2.3.3. Glutathione and cysteine antioxidant consumption assays

The MWCNTs were added to a 2 mM solution of glutathione and cysteine (dissolved in water) in a 12 ml test tube to achieve a final concentration of 1 mM. After incubation for 24 h, the suspensions were filtered to eliminate the MWCNTs and then added to an Ellman reagent solution to a final concentration of 3 mM (Ellman, 1959). The absorbance of the resulting solutions was measured at 410 nm to calculate the amount of unreacted thiols (-SH) using a calibration curve, from which the amount of consumed –SH, corresponding to the consumption of GSH or Cys was derived. For each material, the assays were performed in triplicate.

2.3.4. N-Dimethyl-4-nitrosoaniline assay for quantification of OH° production

The rate of hydroxyl radical generation was determined spectroscopically from the depletion of RNO chemical trap, specific to OH° (Comninellis, 1994). Each MWCNT material was suspended in PBS (2 mM) with 3 mM *N*, *N*-dimethyl-4-nitrosoaniline (dissolved in water). After 24-h incubation, the MWCNTs were filtered out and the absorbance of the remaining solution was measured at 430 nm. A reduction in the absorbance was linearly correlated to the depletion of RNO, which was calculated from the calibration curve. Three independent experiments were conducted for each test material.

2.4. In vitro toxicity tests

2.4.1. Cell culture

The TK6 cells were purchased from ATCC, catalogue number CRL-8015, LOT 17E062. The TK6 cells were incubated at 37 °C in 5 % CO_2 in RPMI (Roswell Park Memorial Institute)-1640 medium (Gibco, USA), which was supplemented with horse serum (HS; Gibco, USA) to a final concentration of 10 % volume/volume, and L-glutamine (2 mM final concentration in the media). Routine sub-culturing was performed to keep the TK6 cells below 1 × 10^6 cells/ml.

Human bronchial epithelial cells 16HBE14o$^-$ (kindly donated by Dr. Grunet, University of California, United States) were cultured in Minimum Essential Medium (MEM) (Gibco, UK) supplemented with 10 % Foetal Bovine Serum (FBS) (Gibco, UK), 1 % penicillin-streptomycin (Gibco, UK) and 1 % L-glutamine (Gibco, UK). The cells were incubated at 37 °C in 5 % CO_2. The culture medium was freshly changed every 2–3 days, and the cells were passaged when they reached 80–90 % confluency in the cell culture treated T-75 flask.

The monocyte-like THP-1 cells were purchased from ECACC (#88081201) and incubated at 37 °C in 5 % CO_2 in RPMI-1640 medium (Biowest, France) supplemented with 10 % FBS, 1 % penicillin-streptomycin and 1 % L-glutamine. The cell suspension was kept between 2 × 10^5–9 × 10^5 cells/ml by adding fresh culture medium as needed. The THP-1 cells were differentiated to macrophage-like (dTHP-1) cells based on the differentiation protocol published by Burgum et al. 2021; supplementing 8 × 10^6 cells in 10 ml RPMI-1640 medium with 50 nM phorbol-12-myristate-13-acetate (PMA, ThermoFisher, Germany) (Burgum et al., 2021). After 24 h incubation, unattached cells (and PMA-media) were removed, cultures were washed with Dulbecco's phosphate-buffered saline solution (DPBS; Biowest, France) and the macrophages were allowed to recover for another 24 h in 15 ml fresh supplemented RPMI-1640 medium.

2.4.2. Mammalian cell gene mutation test

The TK6 cells were first purified with hypoxanthine, aminopterin, thymidine (HAT) (Sigma #H0262) media at 5 × 10^5 cells/ml in 50 ml for 3 days (final concentration of 2 × 10^{-4} M hypoxanthine / 8 × 10^{-7} M aminopterin / 3.5 × 10^{-5} M thymidine), replenishing the media at day two. Briefly, the TK6 cells were centrifuged at 230 *g* for 5 min, washed in 10 ml PBS, and centrifuged again before being resuspended at 4 × 10^5 cells/ml in 50 ml HT medium (Sigma H0137) for 24 h. Following centrifugation at 230 *g* for 5 min, the TK6 cells were resuspended in 200 ml complete RPMI 1640 cell culture media for 3 days, being replenished at day two. Following HPRT mutant cleansing, the TK6 cells were centrifuged at 230 *g* for 5 min and resuspended in fresh culture media at 5 × 10^5 cells/ml (10 ml volume) in T25 flasks for exposure. The TK6 cells were exposed to relevant MWCNTs, negative control (media only) and the positive control methyl methanesulfonate (MMS at 1.5 μg/ml) for 24 h in T25 flasks. Following the exposure, the TK6 cells were centrifuged at 230 *g* for five minutes and re-suspended in 10 ml PBS. The TK6 cells were then suspended in 10 ml of fresh culture media and incubated at 37 °C with 5 % CO_2. The TK6 cells were then maintained at a concentration of 1.25 × 10^5 cells/ml (at 10 ml), being routinely passaged on days 1, 3, 5, 7-post exposure. On day 9 and 11 the volume was increased to 20 ml and 50 ml of complete cell-culture media, respectively. At day 13 post-exposure, cell stocks were prepared for each sample group at 4 × 10^5 cells/ml (100 ml volume) for mutation frequency plating, and 200 cells/ml for plating efficiency, this was sufficient to plate x10 MF and x10 PE for each sample group. Immediately prior to plating of mutation frequency plates, 6-TG (Sigma, A4882) was added for a final concentration of 0.6 μg/ml. The 96-well plates were then incubated undisturbed at 37 °C with 5 % CO_2 for 14 days. After 14 days incubation, the plates were scored for colony formation (Eq. 1–4). MWCNT interference was not detected during the scoring of the live colonies at the end of the experiment.

$$\text{Plating Efficiency\%(PE)} = -\text{Ln}\,(X_o/N_o) \times 100 \quad (1)$$

$$\textit{Cell Viability}\ (\%) = \frac{PE}{PE\ of\ control} \times 100 \quad (2)$$

$$\text{Mutant Frequency (MF)} : MF = \frac{-Ln\left(\frac{X_s}{N_s}\right)}{-Ln\left(\frac{X_o}{N_0}\right)} \text{ x DF} \quad (3)$$

$$\text{Dilution factor (DF)} = \frac{(No.of\ initial\ cells\ per\ well)\ non-selective\ conditions}{(No.of\ initial\ cells\ per\ well)\ selective\ contitions} \quad (4)$$

Whereby the selective conditions were labelled as: X_S=Number of wells without colonies, N_S = Total number of wells (non-selective conditions). X_0 = Number of wells without colonies and N_0 = Total number of wells.

2.4.3. Cytokinesis-blocked micronucleus (CBMN) assay

Monocultures of 16HBE14o$^-$ cells were grown and treated in the

same way as described below for co-cultures, except for the immunostaining of the cells, which was not required. Instead, monocultured cells were fixed with (5:1) methanol: acetic acid and stained with acridine orange and DAPI for the micronucleus analysis as described in Aimonen *et al* in 2021 (Aimonen et al., 2021). A co-culture lung cell model, comprised of 16HBE14o$^-$ cells and dTHP-1 macrophages, was used and it was constructed as previously described (Evans et al., 2019). Prior the co-culture construction, 16HBE14o$^-$ cells were seeded on 6-well plates (2×10^6 cells/well) and cultured for 6 days. Then, 1×10^5 dTHP-1 cells, previously detached by incubating for 10 min with Accutase® (Gibco, UK), were seeded on top of the 16HBE14o$^-$ layer and allowed to adhere for 90 min. Subsequently, 2 ml RPMI was added to the wells and the co-culture system was allowed to stabilize for 24 h. Co-cultured cells were then exposed for 24 h to five doses (6.25, 12.5, 25, 50 and 100 μg/ml) of the NanoGenoTox and high-shear-mixing dispersed MWCNTs. The concentration range applied for this assay was derived from the OECD Guidance Document No. 359 and subsequent publication by Burgum *et al* on the adaptation of OECD TG No. 487 for use with nanomaterials (OECD, 2022; Burgum et al., 2024). Untreated cultures and cultures treated with 0.01 μg/mL of the positive control Mitomycin C (MMC; Sigma-Aldrich, Germany) were included in all experiments. All co-cultures were prepared in duplicate. After exposure, the media was removed, the cultures were washed three times with DPBS, and fresh media containing 3 μg/mL of cytochalasin-B (Sigma-Aldrich Chemie, Germany) was added to the co-cultures for 44 h to induce binucleation of dividing cells. Then, cultures were washed three times with DPBS and detached by incubating 10 min with 1 ml trypsin-EDTA (Gibco, UK). Trypsinization was deactivated by adding 4 ml of supplemented RPMI and the cells were collected into tubes. The remaining cell suspension was centrifuged for 6 min at 210 *g*, and the cell pellet was resuspended in 5 ml of cold supplemented RPMI. The samples were kept on ice and microscope slides were prepared using a Cytospin 4 (Thermo Fisher Scientific, Waltham, MA, USA) for 5 min at 600 rpm. The cells were fixed with 3 % paraformaldehyde in PBS (Sigma-Aldrich, Germany; 15 min), permeabilized with 0.2 % triton-X100 in PBS (ThermoFisher Scientific, USA; 25 min), and pre-treated with 10 % BSA in PBS (Sigma-Aldrich, Germany; 30 min) to prevent non-specific attachment of the antibody.

The samples were then stained with anti-human CD324-FITC (20 μg/ml; BioLegend, USA) and anti-human CD14-PE/Dazzle 594 (1 μg/ml; BioLegend, USA) antibodies, which identify 16HBE14o$^-$ and dTHP-1 cells, respectively. Thereby only the 16HBE14o$^-$ cells expressing E-cadherin fluoresce *via* the CD324-FITC antibody would be scored for micronuclei and the calculation of CBPI (cytokinesis-blocked proliferation index). The antibodies were diluted in PBS with 1 % BSA and samples were stained overnight in the dark at 4 °C. The slides were then washed in PBS and the nuclei stained with 4,6-diamidino-2-phenylindole (DAPI, 0.5 μg/ml) for 5 min, rinsed in tap water, and allowed to dry. The slides were mounted with Vectashield (Vector Laboratories, Inc. Burlingame, CA, USA) and stored at 4 °C in the dark. The slides were coded for blind analysis with all subsequent analyses performed by a single scorer. For micronucleus identification, one thousand 16HBE14o$^-$ binucleated cells per replicate were scored (2000 binucleated cells per dose) using a ZEISS Axio Imager Z1 fluorescent microscope (Carl Zeiss AG, Oberkochen, Germany) and DAPI/FITC/TexasRed triple filter (ChromaTechnology Corp., USA). Cell proliferation was analysed alongside micronucleus scoring to assess the possible effect of the treatments on cell cycle delay (cytostatic effect), to ensure that the treatments were conducted at appropriate levels of cytotoxicity. Cellular cytostasis was calculated from 100 cells per replicate culture (200 cells per dose) based on the cytokinesis-blocked proliferation index (CBPI) (OECD, "Test No., 2016). No MWCNT interference (physical obstruction of micronuclei in binucleated cells) was observed during the scoring of monoculture or co-cultured models. The CBPI, cytostasis, and replication index (RI), a measure of the proliferation rate of the cells, were calculated as follows (Eq. 5–7):

$$\text{Cytokinesis}-\text{blocked proliferation index (CBPI)} = [(\text{No.mononucleate cells}) + 2 \times (\text{No.binucleate cells}) + 3 \times (\text{No.Multinucleate cells})]/(\text{total No.cells}) \quad (5)$$

$$\text{Cytostasis (\%)} = 100\text{–}100[(\text{CBPI}_{\text{Treated}} - 1)/(\text{CBPI}_{\text{Control}} - 1)] \quad (6)$$

$$\text{Replication index (\%) (RI)} = 100\text{–Cytostasis} \quad (7)$$

2.4.4. Evaluation of cellular uptake by transmission electron microscopy

To investigate MWCNT internalisation into 16HBE14o$^-$ cells following the exposure period, transmission electron microscopy (TEM) was utilised. The 16HBE14o$^-$ cells were first exposed to each HARN at 6.25 μg/ml and then; fixed, embedded, sectioned and imaged as previously described (Wills et al., 2016). The same procedure and methodology was applied to the TK6 cells following a 24-h exposure to 20 μg/ml of each respective HARN. The image analysis was performed using the Thermo Scientific Talos F200X scanning/transmission electron microscope (S/TEM) which combines high-resolution STEM and TEM imaging with energy dispersive X-ray spectroscopy (EDX / EDS) signal detection. An Oxford Instruments INCA 350 EDX system/80 mm X-Max SDD detector was used to measure the EDX spectra and the images were captured on a Gatan Orius SC600A CCD camera.

2.5. Statistical analysis

All data sets are presented as the averages +/− the standard deviation. The gene mutation data was analysed using GraphPad Prism version 8.4.3 (GraphPad, USA). The gene mutation data was normally distributed and so a one-way ANOVA with post-hoc Dunnett's was applied to statistically analyse dose-responses against the negative control. The positive control was statistically compared to the negative control using a student's *t*-test. The reactivity of MWCNT was analysed by two-way ANOVA to determine the effect of MWCNT type (NM-400 or NM-401) and dispersion approach for the oxidative potential.

3. Results

3.1. Physico-chemical characterisation

An extensive breakdown of the full physico-chemical characterisation for both the NM-400 and NM-401 used in this study is available from the JRC (Rasmussen et al., 2014). Briefly, the major differences between the two MWCNTs have been summarised in Table 1. NM-401 possesses a slightly higher purity and porosity compared to NM-400, and is significantly longer and wider in diameter, resulting in a very low specific surface area. In addition, X-ray diffraction (XRD) data indicates that graphite may be present in NM-401, and transmission electron microscopy (TEM) reveals that NM-400 is highly curved, while NM-401 possesses a straight and thicker geometry.

Due to the presence of impurities, mainly in NM-400, but also in NM-401, a study on the dissolution rates of the main trace elements was conducted in Milli-Q water to understand their possible release following dispersion. The MWCNTs were filtered after dispersion, and

Table 1
Summary of the primary physico-chemical characterisation data of the reference MWCNTs published in the JRC repository online. The elemental compositions were calculated by EDS measurements.

MWCNT	Length (nm)	Diameter (nm)	Specific Surface Area (m^2/g)	Pore Volume (mL/g)	Purity (%)	Trace elements concentration
NM-400	846 ± 446	11 ± 3	254	0.9613	89.1	Al (46,100 ppm), Si (400 ppm), Fe (7600 ppm), Co (2500 ppm), Cu (2000 ppm), Zn (1900 ppm), O (4.15 wt%)
NM-401	4048 ± 2371	67 ± 24	140	0.0776	99.2	Si (500 ppm), Cu (2300 ppm), Zn (2200 ppm), O (0.6 wt%)

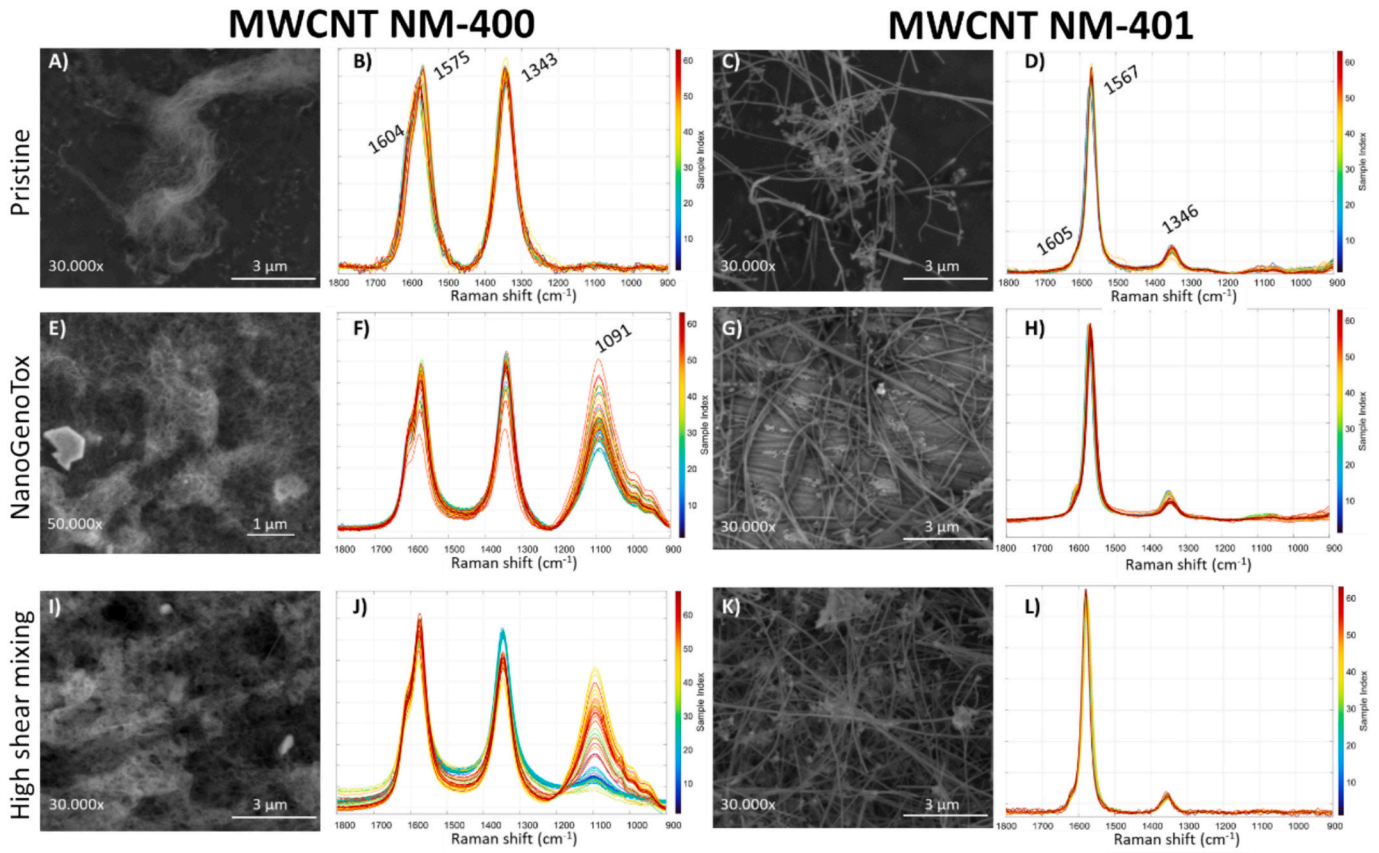

Fig. 1. Scanning electron micrograph (SEM) images and Raman spectra of MWCNT NM-400 (left) and MWCNT NM-401 (right). Pristine powder samples; SEM of NM-400 and NM-401 (A and C) with corresponding Raman spectra (B and D). Dried samples from dispersions obtained following the NanoGenoTox protocol; SEM of NM-400 and NM-401 (E and G) with corresponding Raman spectra (F and H). Dried samples from dispersions obtained following the high-shear mixing protocol; SEM of NM-400 and NM-401 (I and K) with corresponding Raman spectra (J and L).

no significant ion release was observed for any of the elements tested *via* Inductively Coupled Plasma Optical Emission spectroscopy (ICP-OES) at 0 and 24 h in the residual solutions compared to the blank. Therefore, the presence of impurities was not correlated with ion release in Milli-Q water. The structure and morphology of the reference MWCNTs were evaluated by Raman spectroscopy and FE-SEM (Fig. 1). Pristine NM-400 (Fig. 1A) is formed by thinner and shorter MWCNTs than pristine NM-401 (Fig. 1C), in agreement with the JRC characterisation data of Table 1. Both pristine materials appeared agglomerated, so no individual HARNs were appreciated. Two typical graphite bands dominate NM-400 Raman spectra (Fig. 1B), in agreement with the JRC and additional literature (Rasmussen et al., 2014; Bokobza and Zhang, 2012; Hiura et al., 1993). The G band at 1575 cm^{-1}, assigned to in-plane vibration of sp2 hybridized C—C bonds, with a shoulder at 1604 cm^{-1}, and *D* band at 1343 cm^{-1}, assigned to carbon system disorders. In NM-401 spectra, the G band appeared shifted to 1567 cm^{-1} and the D band at 1346 cm^{-1} (Fig. 1D). Moreover, due to the low intensity of the latter, the ratio I_D/I_G is significantly lower for NM-401, which is indicative of a more graphitic structure and a lower number of walls in the MWCNT (Rasmussen et al., 2014). In fact, the NM-401 spectrum resembles the spectra of single wall carbon nanotubes reported in the literature (Costa et al., 2008; Dresselhaus et al., 2005; Dresselhaus et al., 2002). After NanoGenoTox and high-shear mix dispersion, NM-400 MWCNTs were homogeneously distributed without significant fragmentation (Fig. 1E, I). Nevertheless, a new and intense Raman band at 1091 cm^{-1} related to defects appears in all the spectra for both dispersion methods (Fig. 1F, J), indicating that NM-400 MWCNTs are affected by the procedure, being the ultrasonic treatment of the NanoGenoTox protocol more aggressive than the high-shear mixing, since the 1091 cm^{-1} band is more intense and present in most of the spectra. The NM-401 MWCNTs were also well dispersed, but the NanoGenoTox protocol resulted in some scattered MWCNTs that were not stiff (curved morphology, Fig. 1G), whereas the high-shear mixing resulted in homogeneously straight MWCNTs (Fig. 1K). The band at 1091 cm^{-1} does not grow in the spectra of the dispersed NM-401

sample (Fig. 1D, H, L), indicating that, contrary to NM-400, the structure of these MWCNTs is not significantly affected after dispersion.

Finally, the stability of 1 mg/mL suspensions was evaluated over 24 h using both high-shear mixing and the NanoGenoTox protocol. For NM-400, differences were observed between the two methods after 24 h. The suspension prepared with high-shear mixing remained stable throughout the study, as shown by consistent transmittance and backscattering curves (Supplementary Fig. 1-A). However, the suspension obtained using the NanoGenoTox sonication probe showed destabilization after the first hour, with an increase in transmittance at the bottom of the sample holder due to MWCNTs moving towards the surface (Supplementary Fig. 1-B). This was also reflected in the state of suspension of MWCNT NM-400 after 24 h (Supplementary Fig. 2).

In the case of NM-401, this material showed worse dispersion properties compared to NM-400. Destabilization was observed from the start when applying the CSIC method, with transmittance increasing at the bottom due to MWCNTs floating to the top. Additionally, a slight increase in backscattering at the bottom suggested some dispersion, but the low values indicated a limited number of dispersed MWCNTs (Supplementary Fig. 1-C and 1-D). After 24 h, both transmittance and backscattering curves showed differences between the two methods. Although the transmittance profiles were similar, the values were smaller for the high-shear mixed sample, indicating less aggregation and a more stable dispersion compared to the sonication-treated sample.

3.2. Reactivity characterisation

3.2.1. Glutathione, cysteine and N-Dimethyl-4-nitrosoaniline

Both NM-400 and NM-401 resulted very reactive consuming GSH and Cyst antioxidants and, in the case of NM-400, to a lesser extent, also generating OH°. The oxidation of both GSH and Cys is localised at the —S terminus, a functional group that can be easily oxidized by species other than OH°, the most powerful oxidant that can be found in aqueous environment. As the MWCNTs are filtered out before measuring the absorbance of the Ellman reagent, to avoid any interference, glutathione and cysteine that might be adsorbed at their surface would be removed from the solution, so antioxidant amount could also be depleted *via* adsorption at the surface of the MWCNTs, in addition to oxidation. However, adsorption of a hydrophilic and polar molecule as GSH is very unlikely to occur onto hydrophobic, non-polar carbon-based materials. In previous studies, the reactivity of MWCNTs has been explained with the presence of reactive contaminants used as catalysts for their synthesis. The ICP analysis presented in the previous section, however, did not detect any contaminants. The observed reactivity is more plausibly due to reactive defects formed at the surface of the tubes. Fig. 2 reports the bar plots of glutathione, cysteine and *N*-dimethyl-4-nitrosoaniline consumption by the two types of carbon nanotubes in moles per MWCNT's surface area (plot A) and mass (plot B).

3.2.2. Dithiothreitol

The oxidative potential of the NM-400 suspensions as analysed by DTT consumption assay is very high, as reported in an alternate study (currently in press; Alcolea-Rodriguez et al.,). The DTT consumption was close to that of the hydrogen peroxide positive control, independently of the dispersion protocol (Fig. 3). Differently, no oxidative reactivity is obtained with NM-401 when only magnetic stirring is used for dispersion, probably due to low interaction caused by the high hydrophobicity of the material (during reaction the nanotubes were floating on the surface, with no option to react with DTT). Nevertheless, 40 % of the positive control oxidative reactivity is obtained for the NanoGenoTox-dispersed sample, and it approaches 14 % when the high-shear protocol is used to disperse the sample. This increase could be due to the modification of the nanomaterial by the NanoGenoTox and high-shear dispersion methods, but as the Raman spectra do not show significant modifications, more likely it seems to indicate that the reactivity of NM-401, that is not so oxidant as NM-400, increases with a better dispersion, achieved with the high-shear mixing protocol. The statistical analysis performed by two-way ANOVA revealed a significant effect of both the type of CNT and of the dispersion method on DTT oxidation ($p < 0.001$), indicating that with high-shear dispersion, and particularly with NanoGenoTox dispersion, NM-401 reactivity increases significantly compared to the blank (magnetic stirring), and that NM-400 > NM-401 in terms of oxidative potential.

3.3. Genotoxicity evaluation

3.3.1. In vitro mammalian cell gene mutation assay

To determine the cytotoxic and mutagenic potential of NM-400 and NM-401, TK6 cells were exposed to each material in complete cell culture media. Also, under investigation was the potential effect of the dispersion approach upon the observed mutagenicity, so the NanoGenoTox protocol was compared against the high shear dispersion. Following 24 h exposure to NM-400 and NM-401, no statistically significant cytotoxicity or mutagenicity was observed at any test concentration up to 20 μg/ml (Fig. 4) and regardless of the dispersion protocol applied. The positive control of MMS induced a strong, statistically

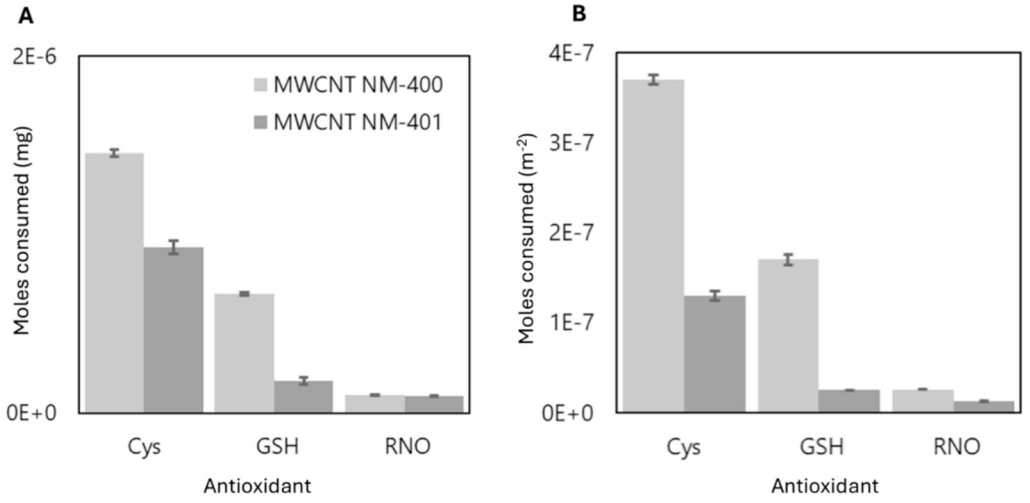

Fig. 2. Consumption of antioxidants (glutathione (GSH), cysteine (Cys)) and depletion of N-dimethyl-4-nitrosoaniline (RNO) (as a measure of generation of OH° radicals). The data is reported as moles per mg (A), and mols per square meter (B) of the tested MWCNTs: NM-400 (light grey) and NM-401 (dark grey). Three independent experiments were conducted.

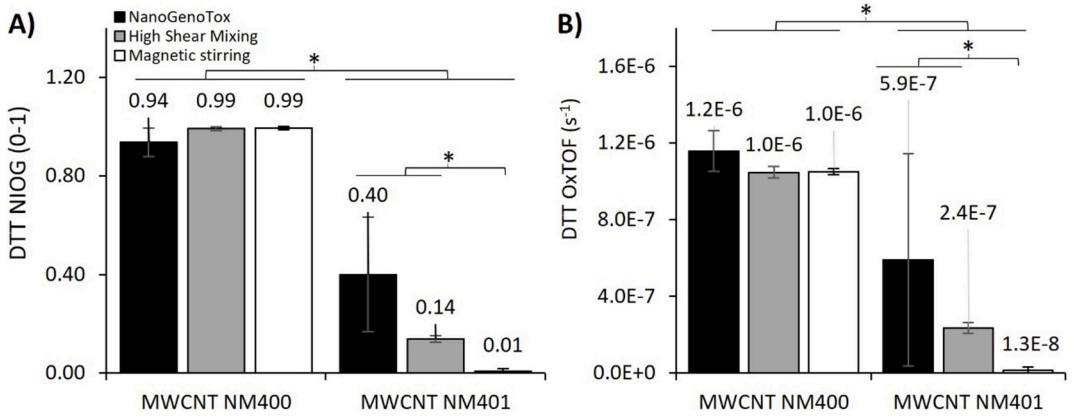

Fig. 3. DTT oxidation reactive descriptors for NM-400 and NM-401. Left (A), normalized index of oxidant generation (NIOG), obtained from DTT conversion. Right (B), oxidative reaction rate normalized per active site, OxTOF. Three independent experiments were conducted. The statistical analysis performed by two-way ANOVA revealed a significant effect of both the type of MWCNT and of the dispersion method on DTT oxidation (*p < 0.001).

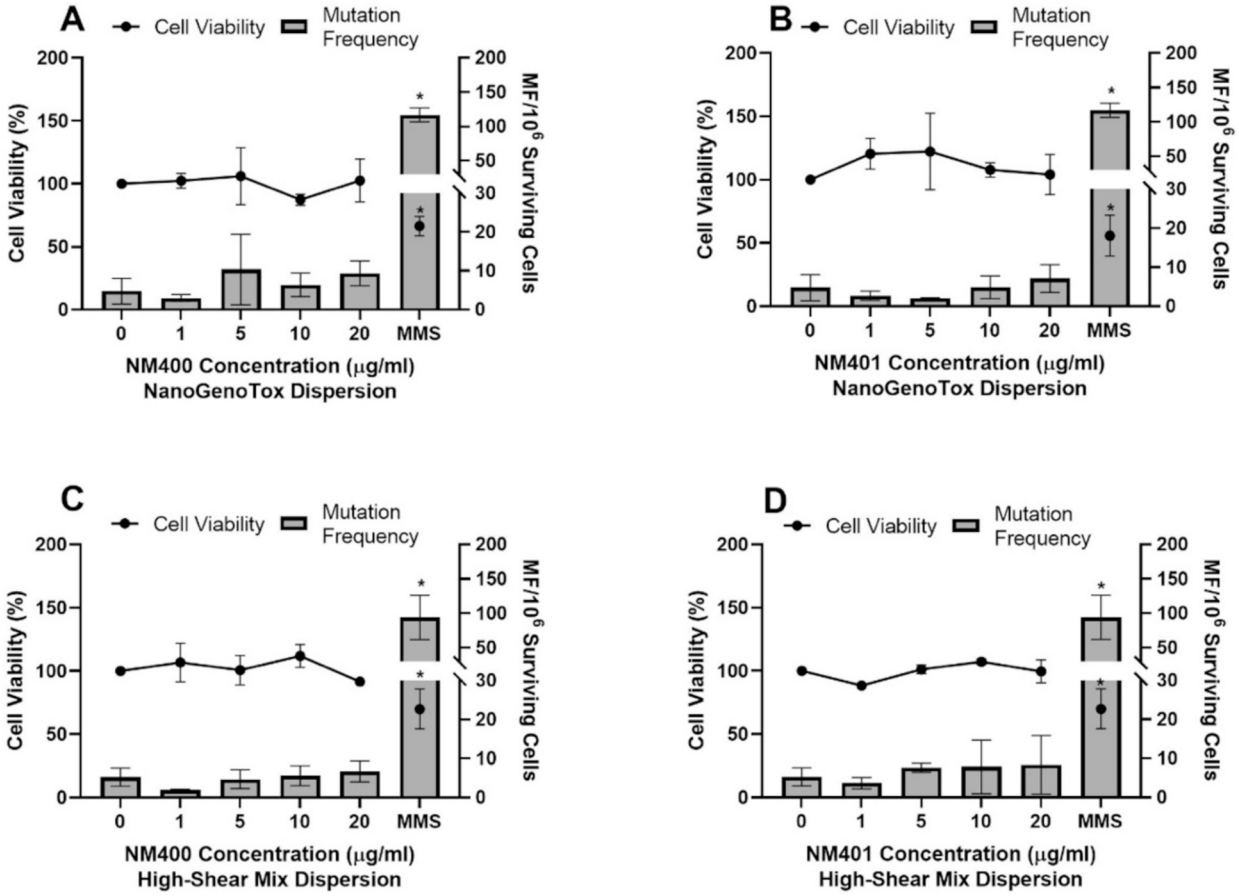

Fig. 4. Cell viability and mutation frequency (MF) in TK6 cells following a 24 h exposure to NM-400 (left) and NM-401 (right). The NM-400 and NM-401 CNTs dispersed using the NanoGenoTox dispersion protocol are represented in A and B respectively. The NM-400 and NM-401 dispersed by high shear mixing are represented in C and *D* respectively. A positive control of MMS was used throughout at a concentration of 1.5 μg/ml. The data represents the average ± the standard deviation. The data was considered statistically significant (*) when the alpha was set at $p \leq 0.05$ ($n = 3$).

significant, response in the TK6 cells, with ~9-fold increases over background levels. An investigation into the cellular uptake of NM-400 and NM-401 by S/TEM showed no internalisation of the HARNs used in the present study at 20 μg/ml (electron micrographs not shown due to the presence of scratches present on the 70 nm sections).

3.3.2. *In vitro cytokinesis-blocked micronucleus assay*

To evaluate primary genotoxicity induced by NM-400 and NM-401, a monoculture of 16HBE14o$^-$ cells were exposed to each material for 24 h. Subsequently, a co-culture of 16HBE14o$^-$ and dTHP1 macrophages was exposed for 24 h to investigate secondary mechanisms (mediated by a (pro)-inflammatory response) of genotoxicity. Fig. 5 shows the results of chromosome damage induction by both reference CNTs for each of the culture systems (co-culture *vs.* monoculture) and dispersion methods (NanoGenoTox *vs.* high shear mix). No reduction in RI below 45 ± 5 % of the concurrent negative control – corresponding to 55 ± 5 % of

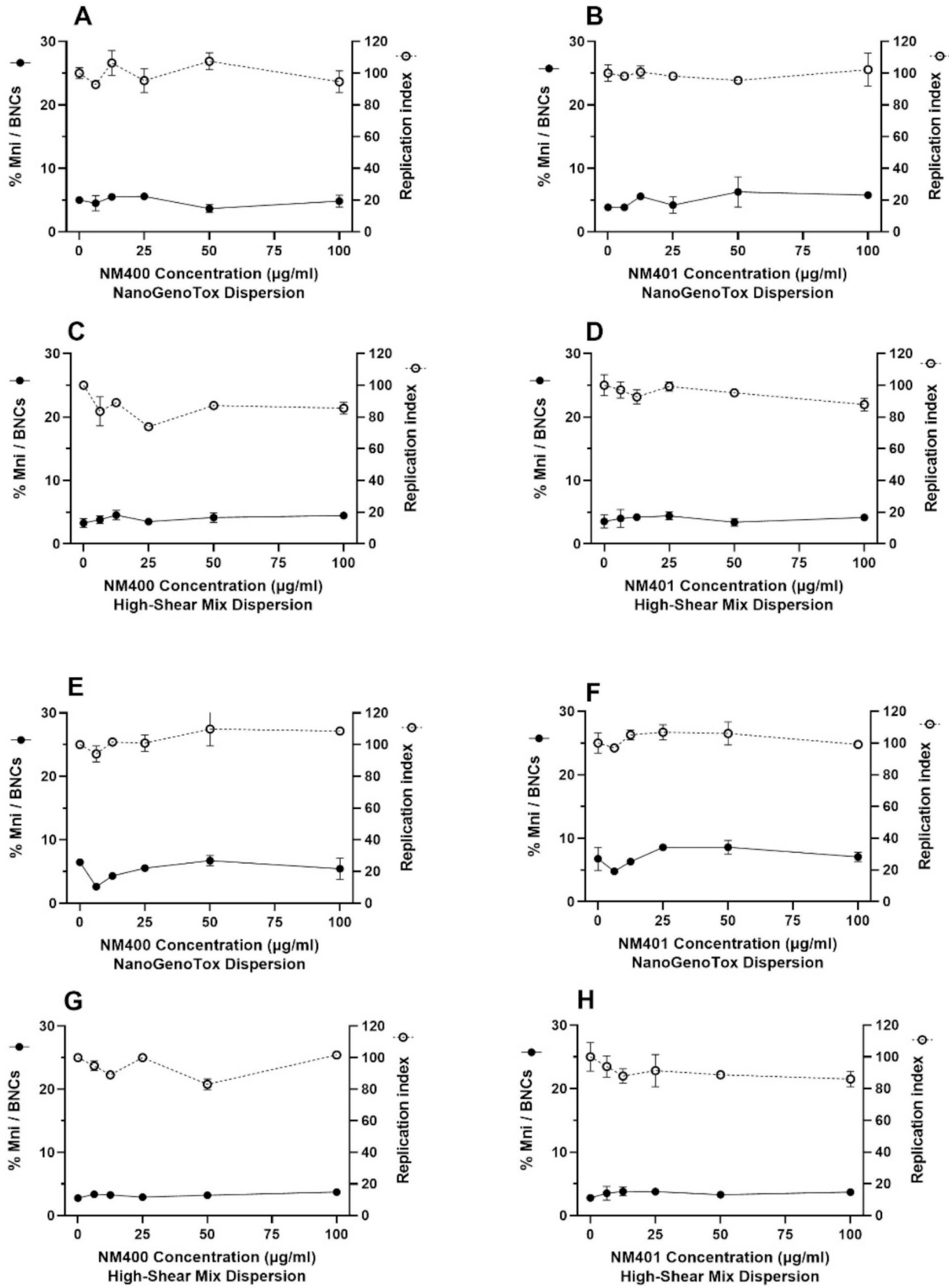

Fig. 5. Chromosomal damage in monocultured 16HBE14o- cells (A-D) and co-cultured 16HBE14o- with dTHP1 cells (*E*-H). Data represents the damage induced by 24 h exposure to NM-400 (left) and NM-401 (right) dispersed following the NanoGenoTox (A-B, E-F) or high-shear mixing (C—D, G-H) protocols. The positive control, MMC (0.01 µg/ml), induced a 3.57 ± 1.42 -fold increase over the negative control values ($p \leq 0.05$). Abbreviations used; Mni / BNCs – number of micronuclei in binucleated cells represented as a percentage. Two independent replicates were conducted.

cytotoxicity as set by the OECD guidelines - was induced by any of the CNTs at the tested doses. Hence, the upper cytotoxicity limit set by the guidelines was not exceeded (OECD, "Test No., 2016). Moreover, none of the CNTs induced a significant increase in the percentage of micronuclei in 16HBE14o$^-$ cells when cultured alone or co-cultured with dTHP-1 cells, regardless of the dispersion method used. The high-shear method generated more stable dispersions than the NanoGenoTox method, resulting in lower intra-dose variability. Further to the lack of genotoxic response, a S/TEM investigation of cellular uptake revealed no MWCNTs present inside the 16HBE14o$^-$ cells (Supplementary Information Fig. 3).

4. Discussion

This study addresses, using OECD-validated methods, the potential genotoxicity of two types of HARNs, NM-400 and NM-401, each with its own unique physico-chemical characteristics. Additionally, the impact of the dispersion protocol used prior to exposure was investigated.

4.1. Effect of the dispersion protocol

The agglomeration of NM-400 observed in this study before and after dispersion is in line with the observations reported by Alig *et al* (Alig et al., 2012). Moreover, the clusters of nanotubes in NM-400 are expected to behave as a single long and wide nanotube (Krause et al., 2009; Dumit et al., 2024). An additional issue is the alteration of the MWCNTs shape and structure by the dispersion protocol. The growth of the 1091 cm^{-1} Raman band observed after both dispersion protocols is related to the formation of structural imperfections. Moreover, as in previous evaluations of the MWCNTs' structure, bands in the 400–1200 cm^{-1} range, known as Intermediate Frequency Modes (IFMs), arise due to the presence of defects. These IFMs suggest a complex interaction influenced by structural imperfections (Saito et al., 2011). NM-401 has been identified as a straight and rigid HARN with physicochemical properties similar to those of the carcinogenic Mitsui XNRi-7 (Poulsen et al., 2015). Conversely, the microscopic examination of NM-400 qualitatively confirmed the absence of structural rigidity coupled with its inability to induce frustrated phagocytosis Moreover, NM-400 was completely engulfed by macrophages isolated from bronchoalveolar lavage (BAL) fluid following *in vivo* exposure in mice, which may be one reason for its comparatively lower capacity to induce genotoxicity (Murphy et al., 2022).

4.2. Reactivity differences observed in NM-400 and NM-401

The comparison of the MWCNTs' reactivity is not straightforward, but DTT oxidation and OH radical generation were always higher for NM-400, independently of the dispersion method and the probe molecule. This could be correlated with the easy formation of structural defects observed by Raman spectroscopy upon NM-400 dispersion following the NanoGenoTox and high-shear mixing protocols, which does not happen for NM-401. Recent works with NM-401 demonstrated no ROS generation when tested with $DCFH_2$, according to the low RNO and DTT consumption of this MWCNT (Murphy et al., 2022). However, NM-400 was found to significantly elevate ROS concentration in the cytochrome C assay (Bengalli et al., 2023). This high reactivity of NM-400, according to thiols consumption and ROS generation, is not correlated in the literature, as the viability of relevant cell lines like A549 and PMA treated THP-1 were not affected at concentrations up to 160 μg/mL for 24 h (Di Ianni et al., 2021). The exception was observed in the study by Bengalli *et al*, who showed a significant decrease of A549 viability at 100 μg/mL (Bengalli et al., 2023). These values are far from those of other benchmark nanomaterials with spherical shapes, whose high surface reactivity induces reactivity-triggered toxicity in these cell lines, as is the case for copper oxide (CuO) and other JRC engineered nanomaterials (ENMs), such as zinc oxide (ZnO) NM-110 and ZnO NM-111 (Alcolea-Rodriguez et al., 2024a).

The high reactivity of MWCNT has previously been associated to the presence of impurities (Nymark et al., 2014). In the present study, the structural defects observed in the Raman spectra for NM-400, and lack of ions release, may correlate the high reactivity with the surface defects. In line with the literature, this reactivity is not reflected by *in vitro* toxicological data in the literature (Darne et al., 2019; Arts et al., 2016). Therefore, it is expected that the toxicity of MWCNT NM-400 may arise from its shape rather than its reactivity (Knudsen et al., 2019). The meta-analysis of integrated proteomic and transcriptomic data by Dumit *et al,* reveals that NM-400 produces cellular changes similar to those caused by rigid carbon fibers, even though according to its dimensions it is classified as non-pathogenic (Dumit et al., 2024).

4.3. In vitro genotoxicity of CNTs

In the present study there was no evidence of statistically significant genotoxicity induced by NM-400 or NM-401 at any test concentration. Whilst some formulations of MWCNTs, such as MWCNT-7, have been shown to be genotoxic (*in vitro* and *in vivo*), there is less compelling evidence to support this for NM-400 and NM-401. What studies with NM-400 typically report, but also with other formulations of MWCNTs, is that oxidative stress-induced DNA damage takes place even at low concentrations, but not or low mutagenicity is induced (Borghini et al., 2017). When specifically looking at the induction of micronuclei, some studies suggest a dose-dependent genotoxicity of NM-400. For instance, Muller *et al* showed that exposure to 10 μg/ml induced significant micronuclei formation in rat lung epithelial cells (two-fold at 50 μg/ml), which was attributed to both clastogenic and aneugenic damage (Muller et al., 2008). More recently, the lack of NM-400 genotoxicity has been reported in a study with a lung co-culture of A549/THP-1a and lung fibroblasts in an air-liquid interface approach. Under monoculture submerged conditions there were only statistically significant increases in %Tail DNA (measured using the comet assay) at excessively high concentrations of 160 μg/ml (Di Ianni et al., 2021).

Few studies observed a mutagenic risk posed by MWCNTs at the HPRT locus. However, a 2016 study by Rubio *et al* reported that Chinese hamster lung fibroblast (V79) cell line successfully internalised NM-401 dispersed using the NanoGenoTox protocol, and DCFH-DA fluorescence showed that the material induced ROS, which was concentration-dependent up to and including the highest concentration of 12 μg/cm^2. In the present study no cellular uptake was observed for TK6 cells or the 16HBE14o$^-$ cell line suggesting cell line-specific uptake in the fibroblasts utilised by Rubio *et al,* which may then explain the positive response the authors observed in the gene mutation assay.

They also reported a cytotoxic effect using the relative growth assay and plating efficiency at 24-h ($p \leq 0.05$ at 15–75 μg/cm^2), 48-h ($p \leq 0.05$ at 15–75 μg/cm^2) and 72-h ($p \leq 0.05$ at 15–75 μg/cm^2) exposure. Statistically significant gene mutation was reported following 24 h exposure at NM-401 concentrations of 0.6, 3, 6 and 12 μg/cm^2. Whilst the gene mutation did not reach the same level as the MMS positive control, there was still a biologically relevant two-fold increase over the untreated control cells (Rubio et al., 2016). Studies evaluating NM-401 with the *in vitro* micronucleus assay in the literature appear to be conflicting with one study reporting that in monocultured BEAS-2B cells genotoxicity can be seen between 5 and 50 μg/ml (García-Rodríguez et al., 2019). However, these results are countered by other studies which show unaltered levels of micronuclei in BEAS-2B cells (Louro et al., 2016). In a separate study, Asakura *et al* exposed female Chinese hamster (CHL/IU) cells to MWCNT-7 (length = 5 μm and width = 88 nm) for 24 h at concentrations between 6 and 100 μg/ml, reporting no statistically significant mutagenicity at the HPRT locus, but significant cytotoxicity – 21 % at the highest concentration (Asakura et al., 2010). Within the study, other DNA damage assays did demonstrate positive responses, highlighting the advantage of utilising a test battery to cover a range of damages that may be induced by these HARNs. For instance,

significant responses were reported for the *in vitro* micronucleus assay at 0.31, 1.3 and 5 μg/ml, as well as significant chromosomal aberrations following 24-h and 48-h exposure at 5, 20 and 80 μg/ml (Asakura et al., 2010). Using the gene mutation assay and the CBMN assay, Manshian *et al* reported statistically significant mutagenicity for a suspension of human lymphoblastoid B (MCL-5) cells and human lung epithelial (BEAS-2B) cells following 24-h exposure to SWCNTs with 1–2 nm in diameter and 1–3 μm in length at 25, 50, and 100 μg/ml, but no mutagenicity was observed with a shorter SWCNT batch (400–800 nm). The response was similar to the positive chemical and HARN controls, N-ethyl-N-nitrosourea (ENU) and crocidolite asbestos, respectively (Manshian et al., 2013).

5. Conclusion

This study demonstrates that NM-400 possesses higher acellular oxidative potential than NM-401 and that the dispersion of NM-400 by sonication or high shear mixing leads to an increase in structural defects and surface reactivity. The effects of the dispersion protocol do not impact MWCNT cellular uptake, nor genotoxicity under the conditions of the present study. When 16HBE14o$^-$ were co-cultured with differentiated THP-1 cells, there appeared to be no evidence of secondary genotoxic mechanisms - regardless of the dispersion approach applied. Thus, the lack of DNA damage indicates that cellular antioxidant defence mechanisms are sufficient to counter the pro-oxidant properties of the dispersed MWCNTs.

Funding

This research has received funding from the European Union's Horizon 2020 research and innovation program for the NanoInformaTIX project, under grant agreement number 814426.

CRediT authorship contribution statement

Michael J. Burgum: Writing – review & editing, Writing – original draft, Visualization, Validation, Software, Resources, Methodology, Investigation, Formal analysis, Data curation. **Víctor Alcolea-Rodríguez:** Writing – review & editing, Visualization, Validation, Software, Resources, Methodology, Investigation, Formal analysis, Data curation. **Hanna Saarelainen:** Visualization, Validation, Software, Resources, Methodology, Investigation, Formal analysis, Data curation. **Raquel Portela:** Writing – review & editing, Visualization, Validation, Supervision, Resources, Project administration, Methodology, Investigation, Funding acquisition, Formal analysis, Conceptualization. **Julián J. Reinosa:** Writing – review & editing, Visualization, Validation, Software, Resources, Methodology, Investigation, Formal analysis, Data curation. **José F. Fernández:** Writing – review & editing, Visualization, Validation, Software, Resources, Methodology, Investigation, Formal analysis, Data curation. **Verónica I. Dumit:** Writing – review & editing, Supervision, Project administration, Methodology, Investigation, Funding acquisition, Conceptualization. **Julia Catalán:** Writing – review & editing, Visualization, Validation, Supervision, Resources, Project administration, Methodology, Investigation, Funding acquisition, Conceptualization. **Felice C. Simeone:** Writing – review & editing, Visualization, Validation, Supervision, Software, Resources, Project administration, Methodology, Investigation, Funding acquisition, Formal analysis, Data curation, Conceptualization. **Lara Faccani:** Visualization, Validation, Software, Resources, Methodology, Investigation, Formal analysis, Data curation. **Martin J.D. Clift:** Writing – review & editing, Visualization, Validation, Supervision, Software, Resources, Project administration, Methodology, Investigation, Funding acquisition, Conceptualization. **Stephen J. Evans:** Writing – review & editing, Software, Methodology, Investigation, Formal analysis, Data curation. **Miguel A. Bañares:** Writing – review & editing, Visualization, Validation, Supervision, Software, Resources, Project administration, Methodology, Investigation, Funding acquisition, Formal analysis, Conceptualization. **Shareen H. Doak:** Writing – review & editing, Visualization, Validation, Supervision, Software, Resources, Project administration, Methodology, Investigation, Funding acquisition, Formal analysis, Conceptualization.

Declaration of competing interest

The authors declare that they have no known competing financial interests or personal relationships that could have appeared to influence the work reported in this paper.

Data availability

The data generated in this manuscript is available from the corresponding author upon reasonable request.

Acknowledgement

The authors would like to acknowledge the Advanced Imaging of Materials (AIM) interdisciplinary facility within the Faculty of Science and Engineering at Swansea University for providing access to the Thermo Scientific Talos F200X scanning/transmission electron microscope (S/TEM).

Appendix A. Supplementary data

Supplementary data to this article can be found online at https://doi.org/10.1016/j.impact.2024.100539.

References

Aimonen, K., et al., 2021. Role of surface chemistry in the in vitro lung response to nanofibrillated cellulose (in eng). Nanomaterials (Basel) 11 (2). https://doi.org/10.3390/nano11020389.

Alarifi, S., Ali, D., 2015. "mechanisms of multi-walled carbon nanotubes-induced oxidative stress and genotoxicity in mouse fibroblast cells," (in eng). Int. J. Toxicol. 34 (3), 258–265. https://doi.org/10.1177/1091581815584799.

Alarifi, S., Ali, D., Verma, A., Almajhdi, F.N., Al-Qahtani, A.A., 2014. "single-walled carbon nanotubes induce cytotoxicity and DNA damage via reactive oxygen species in human hepatocarcinoma cells," (in eng). In Vitro Cell. Dev. Biol. Anim. 50 (8), 714–722. https://doi.org/10.1007/s11626-014-9760-3.

Alcolea-Rodriguez, V., Dumit, V.I., Ledwith, R., Portela, R., Bañares, M.A., Haase, A., 2024a. "differentially induced autophagy by engineered nanomaterial treatment has an impact on cellular homeostasis and cytotoxicity," (in eng). Nano Lett. 24 (38), 11793–11799. https://doi.org/10.1021/acs.nanolett.4c01573.

Alcolea-Rodriguez, V., Portela, R., Calvino-Casilda, V., Bañares, M.A., 2024b. In chemico methodology for engineered nanomaterial categorization according to number, nature and oxidative potential of reactive surface sites. Environ. Sci.: Nano. https://doi.org/10.1039/D3EN00810J.

Aldieri, E., et al., 2013. The role of iron impurities in the toxic effects exerted by short multiwalled carbon nanotubes (MWCNT) in murine alveolar macrophages. J. Toxicol. Environ. Health A 76 (18), 1056–1071. https://doi.org/10.1080/15287394.2013.834855.

Alig, I., et al., 2012. Establishment, morphology and properties of carbon nanotube networks in polymer melts. Polymer 53 (1), 4–28. https://doi.org/10.1016/j.polymer.2011.10.063.

Arts, J.H., et al., 2016. Case studies putting the decision-making framework for the grouping and testing of nanomaterials (DF4nanoGrouping) into practice (in eng). Regul. Toxicol. Pharmacol. 76, 234–261. https://doi.org/10.1016/j.yrtph.2015.11.020.

Asakura, M., et al., 2010. Genotoxicity and cytotoxicity of multi-wall carbon nanotubes in cultured Chinese hamster lung cells in comparison with chrysotile a fibers (in eng). J. Occup. Health 52 (3), 155–166. https://doi.org/10.1539/joh.l9150.

Bengalli, R.D., Zerbi, G., Lucotti, A., Catelani, T., Mantecca, P., 2023. Carbon nanotubes: structural defects as stressors inducing lung cell toxicity (in eng). Chem. Biol. Interact. 382, 110613. https://doi.org/10.1016/j.cbi.2023.110613.

Bokobza, L., Zhang, J., 2012. Raman spectroscopic characterization of multiwall carbon nanotubes and of composites. Express Polym Lett 6 (7), 601–608. https://doi.org/10.3144/expresspolymlett.2012.63.

Borghini, A., Roursgaard, M., Andreassi, M.G., Kermanizadeh, A., Moller, P., 2017. Repair activity of oxidatively damaged DNA and telomere length in human lung epithelial cells after exposure to multi-walled carbon nanotubes (in eng). Mutagenesis 32 (1), 173–180. https://doi.org/10.1093/mutage/gew036.

Burgum, M.J., et al., 2021. Few-layer graphene induces both primary and secondary genotoxicity in epithelial barrier models in vitro (in eng). J. Nanobiotechnol. 19 (1), 24. https://doi.org/10.1186/s12951-021-00769-9.

Burgum, M.J., et al., 2024. Adapting the in vitro micronucleus assay (OECD Test guideline No. 487) for testing of manufactured nanomaterials: recommendations for best practices (in eng). Mutagenesis. https://doi.org/10.1093/mutage/geae010.

C. P. A. Jensen K. A., Birkedal R., Kembouche Y., Christiansen E., Jacobsen N. R., et al, "Towards a Method for Detecting the Potential Genotoxicity of Nanomaterials. Deliverable 3. Final Protocol for Producing Suitable Manufactured Nanomaterial Exposure Media. The Generic NANOGENOTOX dispersion protocol. Standard Operating Procedure (SOP) and Background Documentation, n.d. " pp. 1–33.

Comninellis, C., 1994. Electrocatalysis in the electrochemical conversion/combustion of organic pollutants for waste water treatment. Electrochem. Acta 39 (11–12), 5.

Costa, S., Borowiak-Palen, E., Kruszyñska, M., Bachmatiuk, A., Kaleńczuk, R.J., 2008. Characterization of carbon nanotubes by Raman spectroscopy. Mater. Sci. Pol. 26 (2), 433–441.

Darne, C., et al., 2019. A non-damaging purification method: decoupling the toxicity of multi-walled carbon nanotubes and their associated metal impurities. Environ. Sci.: Nano 6 (6), 1852–1865. https://doi.org/10.1039/c8en01276h.

Di Cristo, L., et al., 2019. Comparative in vitro cytotoxicity of realistic doses of benchmark multi-walled carbon nanotubes towards macrophages and airway epithelial cells (in eng). Nanomaterials (Basel) 9 (7). https://doi.org/10.3390/nano9070982.

Di Ianni, E., et al., 2021. In vitro-in vivo correlations of pulmonary inflammogenicity and genotoxicity of MWCNT. Part. Fibre Toxicol. 18 (1), 25. https://doi.org/10.1186/s12989-021-00413-2.

Dresselhaus, M.S., Dresselhaus, G., Jorio, A., Souza Filho, A.G., Saito, R., 2002. Raman spectroscopy on isolated single wall carbon nanotubes. Carbon 40 (12), 2043–2061. https://doi.org/10.1016/S0008-6223(02)00066-0.

Dresselhaus, M.S., Dresselhaus, G., Saito, R., Jorio, A., 2005. Raman spectroscopy of carbon nanotubes. Phys. Rep. 409 (2), 47–99. https://doi.org/10.1016/j.physrep.2004.10.006.

Dumit, V.I., et al., 2024. Meta-analysis of integrated proteomic and transcriptomic data discerns structure-activity relationship of carbon materials with different morphologies (in eng). Adv. Sci. (Weinh) 11 (9), e2306268. https://doi.org/10.1002/advs.202306268.

Ellman, G.L., 1959. Tissue sulfhydryl groups. Arch. Biochem. Biophys. 82 (1), 70–77. https://doi.org/10.1016/0003-9861(59)90090-6.

Evans, S.J., et al., 2019. In vitro detection of in vitro secondary mechanisms of genotoxicity induced by engineered nanomaterials (in eng). Part. Fibre Toxicol. 16 (1), 8. https://doi.org/10.1186/s12989-019-0291-7.

Fenoglio, I., et al., 2008. Structural defects play a major role in the acute lung toxicity of multiwall carbon nanotubes: physicochemical aspects (in eng). Chem. Res. Toxicol. 21 (9), 1690–1697. https://doi.org/10.1021/tx800100s.

García-Rodríguez, A., et al., 2019. Micronuclei detection by flow cytometry as a high-throughput approach for the genotoxicity testing of nanomaterials (in eng). Nanomaterials (Basel) 9 (12). https://doi.org/10.3390/nano9121677.

Hiura, H., Ebbesen, T.W., Tanigaki, K., Takahashi, H., 1993. Raman studies of carbon nanotubes. Chem. Phys. Lett. 202 (6), 509–512. https://doi.org/10.1016/0009-2614(93)90040-8.

Johnston, H.J., et al., 2010. A critical review of the biological mechanisms underlying the in vivo and in vitro toxicity of carbon nanotubes: the contribution of physico-chemical characteristics (in eng). Nanotoxicology 4 (2), 207–246. https://doi.org/10.3109/17435390903569639.

Knudsen, K.B., et al., 2019. Physicochemical predictors of multi-walled carbon nanotube-induced pulmonary histopathology and toxicity one year after pulmonary deposition of 11 different multi-walled carbon nanotubes in mice (in eng). Basic Clin. Pharmacol. Toxicol. 124 (2), 211–227. https://doi.org/10.1111/bcpt.13119.

Krause, B., Petzold, G., Pegel, S., Pötschke, P., 2009. Correlation of carbon nanotube dispersability in aqueous surfactant solutions and polymers. Carbon 47 (3), 602–612. https://doi.org/10.1016/j.carbon.2008.10.040.

Louro, H., Pinhão, M., Santos, J., Tavares, A., Vital, N., Silva, M.J., 2016. "evaluation of the cytotoxic and genotoxic effects of benchmark multi-walled carbon nanotubes in relation to their physicochemical properties," (in eng). Toxicol. Lett. 262, 123–134. https://doi.org/10.1016/j.toxlet.2016.09.016.

Manshian, B.B., et al., 2013. "single-walled carbon nanotubes: differential genotoxic potential associated with physico-chemical properties," (in eng). Nanotoxicology 7 (2), 144–156. https://doi.org/10.3109/17435390.2011.647928.

Muller, J., et al., 2008. Clastogenic and aneugenic effects of multi-wall carbon nanotubes in epithelial cells (in eng). Carcinogenesis 29 (2), 427–433. https://doi.org/10.1093/carcin/bgm243.

Murphy, F., et al., 2022. Grouping MWCNTs based on their similar potential to cause pulmonary hazard after inhalation: a case-study (in eng). Part. Fibre Toxicol. 19 (1), 50. https://doi.org/10.1186/s12989-022-00487-6.

Nymark, P., et al., 2014. Free radical scavenging and formation by multi-walled carbon nanotubes in cell free conditions and in human bronchial epithelial cells (in eng). Part Fibre Toxicol. 11 (4). https://doi.org/10.1186/1743-8977-11-4.

OECD, 2016. Test No. 476: In Vitro Mammalian Cell Gene Mutation Tests using the Hprt and xprt genes.

OECD, 2022. Study report and preliminary guidance on the adaptation of the in vitro micronucleus assay (OECD TG 487) for testing of manufactured nanomaterials. In: OECD Environment, Health and Safety Publications Series on Testing & Assessment No. 359.

OECD, "Test No., 2016. 487. In: Vitro Mammalian Cell Micronucleus Test, OECD Guidelines for the Testing of Chemicals, Section 4. OECD Publishing, Paris.

Pei, B., Wang, W., Dunne, N., Li, X., 2019. Applications of carbon nanotubes in bone tissue regeneration and engineering: superiority, concerns, current advancements, and prospects (in eng). Nanomaterials (Basel) 9 (10). https://doi.org/10.3390/nano9101501.

Poland, C.A., et al., 2008. Carbon nanotubes introduced into the abdominal cavity of mice show asbestos-like pathogenicity in a pilot study (in eng). Nat. Nanotechnol. 3 (7), 423–428. https://doi.org/10.1038/nnano.2008.111.

Poulsen, S.S., et al., 2015. MWCNTs of different physicochemical properties cause similar inflammatory responses, but differences in transcriptional and histological markers of fibrosis in mouse lungs (in eng). Toxicol. Appl. Pharmacol. 284 (1), 16–32. https://doi.org/10.1016/j.taap.2014.12.011.

G. Rahman *et al.*, "An overview of the recent progress in the synthesis and applications of carbon nanotubes," vol. 5, no. 1, n.d.

Rasmussen, K., et al., 2014. Multi-Walled Carbon Nanotubes, NM-400, NM-401, NM-402, NM-403: Characterisation and Physico-Chemical Properties. Publications Office of the European Union, Luxembourg (Luxembourg), p. 2014.

Rubio, L., El Yamani, N., Kazimirova, A., Dusinska, M., Marcos, R., 2016. Multi-walled carbon nanotubes (NM401) induce ROS-mediated HPRT mutations in Chinese hamster lung fibroblasts (in eng). Environ. Res. 146, 185–190. https://doi.org/10.1016/j.envres.2016.01.004.

Sabido, O., et al., 2020. Quantitative flow cytometric evaluation of oxidative stress and mitochondrial impairment in RAW 264.7 macrophages after exposure to pristine, acid functionalized, or annealed carbon nanotubes (in eng). Nanomaterials (Basel) 10 (2). https://doi.org/10.3390/nano10020319.

Saito, R., Hofmann, M., Dresselhaus, G., Jorio, A., Dresselhaus, M.S., 2011. Raman spectroscopy of graphene and carbon nanotubes. Adv. Phys. 60 (3), 413–550. https://doi.org/10.1080/00018732.2011.582251.

Saliev, T., 2019. The advances in biomedical applications of carbon nanotubes. C 5 (2), 29.

Schnorr, J.M., Swager, T.M., 2011. Emerging applications of carbon nanotubes. Chem. Mater. 23 (3), 646–657. https://doi.org/10.1021/cm102406h.

Wills, J.W., et al., 2016. Genetic toxicity assessment of engineered nanoparticles using a 3D in vitro skin model (EpiDerm) (in eng). Part. Fibre Toxicol. 13 (1), 50. https://doi.org/10.1186/s12989-016-0161-5.

Wils, R.S., Jacobsen, N.R., Di Ianni, E., Roursgaard, M., Møller, P., 2021. Reactive oxygen species production, genotoxicity and telomere length in FE1-Muta™Mouse lung epithelial cells exposed to carbon nanotubes (in eng). Nanotoxicology 15 (5), 661–672. https://doi.org/10.1080/17435390.2021.1910359.